Werk

Jahr: 1982
Kollektion: fid.geo
Signatur: 8 Z NAT 2148:51
Digitalisiert: Niedersächsische Staats- und Universitätsbibliothek Göttingen
Werk Id: PPN1015067948_0051
PURL: http://resolver.sub.uni-goettingen.de/purl?PPN1015067948_0051

LOG Id: LOG_0018
LOG Titel: Observations of ionospheric and field-aligned currents in the late afternoon sector with triad and the Scandinavian magnetometer array
LOG Typ: article

Übergeordnetes Werk

Werk Id: PPN1015067948
PURL: http://resolver.sub.uni-goettingen.de/purl?PPN1015067948
OPAC: http://opac.sub.uni-goettingen.de/DB=1/PPN?PPN=1015067948

Contact

Niedersächsische Staats- und Universitätsbibliothek Göttingen
Georg-August-Universität Göttingen
Platz der Göttinger Sieben 1
37073 Göttingen
Germany
Email: gdz@sub.uni-goettingen.de

J. Geophys. (1982) 51:55–65

Journal of Geophysics

Observations of Ionospheric and Field-Aligned Currents in the Late Afternoon Sector with Triad and the Scandinavian Magnetometer Array

H. Sulzbacher[1], W. Baumjohann[1,2], T.A. Potemra[2], E. Nielsen[3], and G. Gustafsson[4]

[1] Institut für Geophysik der Universität Münster, Corrensstr. 24, D-4400 Münster, Federal Republic of Germany
[2] Applied Physics Laboratory, Johns Hopkins University, Laurel, Md. 20810, USA
[3] Max-Planck-Institut für Aeronomie, D-3411 Katlenburg-Lindau 3, Federal Republic of Germany
[4] Kiruna Geophysical Institute, S-98127, Kiruna, Sweden

Abstract. By using coordinated two-dimensional ground-based and satellite magnetic measurements obtained during a late afternoon sector pass of TRIAD over the Scandinavian Magnetometer Array (SMA) and irregularity drift measurements by the STARE Trondheim radar we were able to deduce ionospheric and field-aligned currents quantitatively. The apparent contradiction – which is often met in the afternoon sector – that the TRIAD measurements indicated upward *net* field-aligned currents whereas the ground-based magnetometers showed the signatures of downward *net* field-aligned currents, was resolved by taking the polar cap current system and the (different) finite east-west extent of the field-aligned current sheets into account. In particular, we found: The most prominent current was a broad eastward Hall current electrojet of about $4 \cdot 10^5$ A whose intensity increased to the east and which was fed by a downward net field-aligned current sheet of about 220 mAm^{-1} which extended about 2,000 km in longitude. The meridional current system in the eastward electrojet region was formed by a northward Pedersen current of about 400 mAm^{-1} and the corresponding balanced field-aligned closure currents in the north and south, with a peak intensity of about 2 μAm^{-2} The strength of the meridional current system also increased to the east. South of the main eastward electrojet, in sunlit subauroral latitudes, a broad but weak (less than 40 mAm^{-1}) current (a so-called UV electrojet) was flowing eastward, while immediately north of the main (eastward) electrojet a narrow westward Hall current of the order of 10^5 A penetrated into the afternoon sector and diverged up the magnetic field lines as a net field-aligned current sheet of about 100 mAm^{-1} Within the polar cap a broad westward Hall current (200–300 mAm^{-1} height-integrated current density) and duskward Pedersen currents of about 120 mAm^{-1} were flowing. Current continuity for the Pedersen currents was provided by about 5,000 km long upward and downward directed field-aligned current sheets of about 120 mAm^{-1} at the dusk and dawn polar cap border, respectively. The Σ_H/Σ_P ratio determined from the magnetic measurements had values around 2 in the eastward electrojet region and was considerably higher in the westward electrojet region. By assuming that the ionospheric electric field had only a meridional component in the afternoon sector, we deduced the two-dimensional distribution of electric field vectors from the STARE Trondheim radar measurements and subsequently could compute height-integrated Hall and Pedersen conductivities. Whereas the electric field decreased towards the south and, more slightly, towards the east, the height-integrated Hall conductivity showed the opposite behaviour.

Key words: TRIAD satellite – Scandinavian Magnetometer Array – STARE radar – Auroral electrojets – Field-aligned currents – Ionospheric conductivities

Reprint requests to. W. Baumjohann

Introduction

It is well known that during periods of enhanced magnetospheric activity an eastward electrojet flows in the afternoon and evening sector along the southern part of the auroral oval (Kamide and Fukushima, 1972; Rostoker, 1972). The eastward electrojet exists simultaneously with a poleward situated westward electrojet, which penetrates from the midnight into the evening sector during periods of substorm activity (Rostoker and Kisabeth, 1973; Rostoker et al., 1975; Mersmann et al., 1979). The westward electrojet can sometimes extend past the dusk meridian (Hughes et al., 1979; Rostoker et al., 1979).

By taking into account the northward electric field observed by satellites (e.g. Maynard, 1974), rockets (e.g. Maynard et al., 1977), balloons (e.g. Mozer and Lucht, 1974) and the Chatanika radar (e.g. Banks et al., 1973) in the eastward electrojet region, it has been argued that the northward magnetic fields observed on the ground in the afternoon and evening sector are caused by eastward flowing Hall currents (e.g. Hughes, 1978; Hughes and Rostoker, 1977; Mersmann et al. 1979; Rostoker, 1979). Baumjohann et al. (1978) and especially Baumjohann (1979) and Baumjohann et al. (1980) could actually verify this for typical cases by comparing simultaneous two-dimensional measurements of ground magnetic and ionospheric electric fields obtained by the Scandinavian Magnetometer Array (SMA) and the Scandinavian Twin Auroral Radar Experiment (STARE), respectively. Moreover, Baumjohann et al. (1980) gave rather direct evidence that the net fieldaligned current flow (Heppner et al., 1971a, b; Yasuhara et al., 1975; Sugiura and Potemra, 1976) above the eastward electrojet region is caused by the divergence of the eastward Hall current due to longitudinal conductivity or electric field gradients, as proposed by Hughes and Rostoker (1977, 1979). To date nobody has reported on electric field measurements in the more poleward situated westward electrojet and thus the nature of this current is as yet rather unclear.

However, since the nearly toroidal magnetic fields of the current circuits formed by Pedersen and balanced field-aligned currents are barely observable on the ground (Boström, 1964; Kamide and Matsushita, 1979a, b; Baumjohann et al., 1980)

0340-062X/82/0051/0055/$02.20

neither Hughes and Rostoker (1977, 1979) nor Baumjohann et al. (1980) were able to determine the parameters of the meridional current systems in the afternoon sector and to compare it with the longitudinal current circuit formed by Hall and net field-aligned currents. The toroidal magnetic field of the meridional current system can be observed, however, by rockets and satellites, flowing above the horizontal currents in the auroral E layer. In fact, Rostoker et al. (1975) and Kamide and Akasofu (1976) compared qualitatively the directions of field-aligned current inferred from TRIAD observations with the regions of eastward and westward electrojets inferred from ground-based measurements by the Alberta and Alaska meridional chains, but they did not take into account longitudinal gradients and got quite different results. Moreover, there is an apparent contradiction that satellite measurements on the average indicated strong upward net field-aligned current in the afternoon sector (e.g. Sugiura and Potemra, 1976, Iijima and Potemra, 1976, 1978) whereas ground-based magnetometers often showed the signatures of downward net field-aligned currents (Hughes and Rostoker, 1977, 1979; Baumjohann et al., 1980).

The aim of the present study is to deduce quantitatively, for a typical single case, the longitudinal and the meridional current circuits in the late afternoon sector of the auroral oval by comparing SMA and TRIAD measurements of magnetic fields and to get a better understanding of the coupling between field-aligned and ionospheric currents. That simultaneous SMA and TRIAD observations form a powerful data set has already been demonstrated for the morning sector westward electrojet by Baumjohann et al. (1979) and Sulzbacher et al. (1980). Moreover, simultaneous measurements of one component of the irregularity drifts in the E region by the STARE Trondheim radar (unfortunately the other STARE radar at Hankasalmi did not work properly during the present event) allowed us to draw some conclusions on the ionospheric electric field and conductivity.

Instrumentation and Data

On 4 January 1979, between 1350 and 1354 UT (around 1630 MLT) the TRIAD satellite traversed the afternoon auroral oval over Scandinavia during a relatively disturbed time (K_P= 5−). The SMA magnetograms showed positive magnetic disturbances lasting for several hours. The disturbance amplitudes changed only slightly during the TRIAD pass. Accordingly, the analyzed current system can be regarded as stationary.

Figure 1 displavs the sites of the magnetic stations used in this study together with the averaged (1350–1354 UT) equivalent current vectors (the observatory at New Alesund, far in the north – 78.9° N, 11.9° E – from which data were used in addition, is not shown here). A full description of the SMA can be found in Küppers et al. (1979) and Maurer and Theile (1978). The equivalent current vectors are given relative to the quiet night level.

Also drawn into Figure 1 are the 10 s averages of the horizontal magnetic field vectors derived from the TRIAD data along the satellite track with the trajectory projected down to 120 km height along magnetic field lines. The TRIAD magnetic field vectors are given relative to a baseline calculated with the algorithm given by Gustafsson et al. (1981). A detailed description of the TRIAD magnetometer may be found in Armstrong and Zmuda (1973). The dashed line denoted T gives the terminator at 120 km altitude.

The coordinate system indicated in Figure 1 was described by Küppers et al. (1979) and was named the Kiruna system.

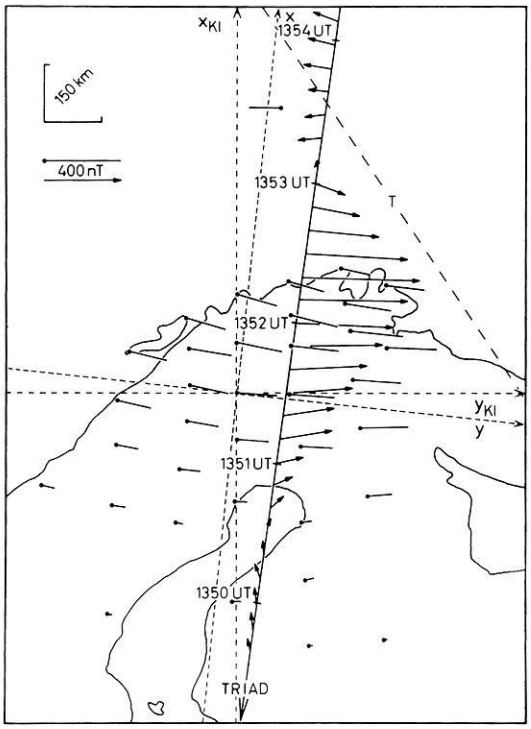

Fig. 1. Four minute averaged equivalent current vectors on the ground and 10 s averaged horizontal magnetic disturbance vectors along the satellite track (projected down along the field lines to 100 km). Also indicated are the axes of the Kiruna system and of the rotated (x, y) system which are explained in the text. The *dashed line* denoted by T gives the terminator at 120 km height

It is a Cartesian coordinate system obtained by a stereographic projection of the globe onto a tangential plane centered at Kiruna, Sweden. The y_{KI} axis of the system has been chosen as the tangent to the revised corrected geomagnetic latitude circle (after Gustafsson, 1970) running through Kiruna (64.8°). The x_{KI} axis points approximately 12° west of geographic north at Kiruna. In order to simplyfy the first interpretation of the data and the model calculation we rotated the Kiruna system by 6° clockwise around the vertical z axis and obtained x and y axes which are othogonal and parallel to the direction of the electrojets, respectively (see Fig. 1). In the following we will denote the magnetic components measured on the ground parallel to x, y and z axes as A_M, B_M and Z_M, respectively, and those measured by TRIAD as A_T, B_T and Z_T. Of course, the results of the model calculation are independent of the coordinate system chosen.

Unfortunately, during the present event only one of the STARE radars (Greenwald et al., 1978) worked properly: the Trondheim radar measured the two-dimensional distribution of one component of the irregularity drift vectors with an integration time of 1 min. We calculated running averages over three data points from a given beam and used every second average, which yielded a spatial resolution of about 30–40 km.

Description of the Current System

The equivalent current vectors in Figure 1 show an eastward electrojet over the Scandinavian peninsula, in the same region where the satellite magnetic field is also eastward directed. North of the eastward electrojet flows a westward equivalent current, and here the magnetic disturbance vectors measured by TRIAD are also westward directed.

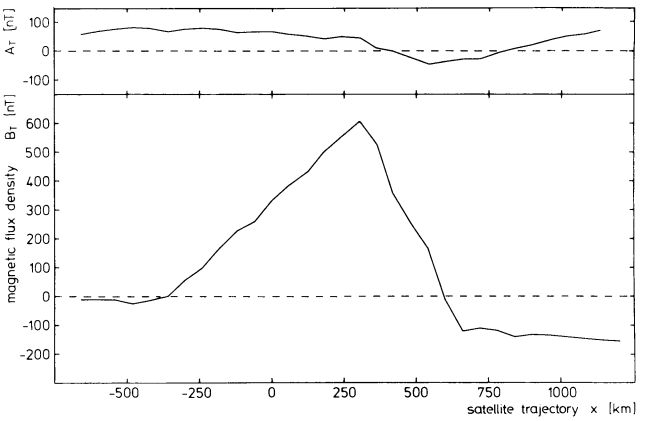

Fig. 2. Ten seconds averaged (about 60 km) horizontal magnetic components observed by TRIAD after baseline reduction, projection down to ionospheric heights and transformation into the (x, y) system. A_T and B_T are parallel to x and y, respectively

Since SMA equivalent current vectors and TRIAD magnetic field vectors are nearly parallel, we can follow, for example, Boström (1964), Anderson and Vondrak (1975), Untiedt et al. (1978), and Mallinckrodt and Carlson (1978), in assuming that the eastward electrojet and the westward current to the north are Hall currents driven by northward and southward electric fields, respectively, of magnetospheric origin. Additionally northward and southward Pedersen currents must flow in the eastward electrojet and westward Hall current region, respectively, which together with the associated balanced field-aligned currents form the meridional current system.

The assumption of a northward directed electric field in the southern part of the afternoon auroral zone is strongly suggested by the results of numerous other measurements (Mozer and Lucht, 1974; Banks and Doupnik, 1975; Madsen et al., 1976; Holzworth et al., 1977; Horwitz et al., 1978a, b; Baumjohann et al., 1980; Zi and Nielsen, 1980), and concurs also with the westward irregularity drift components measured by the Trondheim radar (the irregularities measured by the STARE radars are ExB drifting; see Greenwald, 1979). The assumption of a southward electric field in the westward current region (and in the polar cap – see below) is consistent with the typical dawn-to-dusk electric field configuration at high latitudes (Heppner, 1972, 1973, 1977; Maynard 1974; Heelis and Hanson, 1980).

The A_T and B_T components measured by TRIAD at about 850 km altitude and projected down along magnetic field lines to 100 km height are displayed in Figure 2. A two-dimensional calculation of the field-aligned current density (positive downward) according to

$$j_{\shortparallel}(x)=\mu_0^{-1}\frac{\partial B_T(x)}{\partial x} \tag{1}$$

shows immediately that the latitudes between $x=-500$ km and $x=+300$ km are covered by downward field-aligned currents while between about $x=+300$ km and $x=+660$ km a twice as intense field-aligned current flows upward. The level shift seems to indicate that between $x=-500$ km and $x=+660$ more current flows upward than downward (cf. Sugiura and Potemra, 1976). The significant A_T component clearly shows that the current system is three-dimensional (cf. Sulzbacher et al., 1980).

The (time averaged) A_M, B_M and Z_M latitude profiles along the x axis are shown in Figure 3. The Z_M and especially the A_M components (note the different scale) indicate that the eastward electrojet increases from the west (profile 1) to the east up to profile 5 and then probably stays about constant (profile 6). The westward equivalent current in the polar cap (here defined as the region where no field-aligned currents flow) probably constitutes a part of the two-cell convection as described by Friis-Christensen and Wilhjelm (1975) and Nagai and Fukushima (1979). The model calculations following in the next section will show that the strongly negative Z_M components around $x=500$ km can only be explained by a latitudinally narrow but strong westward ionospheric current just north of the eastward electrojet. This current can probably be regarded as the substorm-associated westward electrojet which often penetrates deep into the evening and even into the afternoon sector (Wiens and Rostoker, 1975; Rostoker et al., 1975; Horwitz et al. 1978b, Mersmann et al., 1979 and Hughes et al. 1979). This same westward ionospheric current diverges upward as a net field-aligned current at its western end (Hughes and Rostoker, 1979; Rostoker and Hughes, 1979).

Assuming vertical magnetic field lines the net field-aligned currents are related to the longitudinal Hall currents as follows:

$$J_{\shortparallel}(x, y)=\frac{\partial J_y(x, y)}{\partial y} \tag{2}$$

Hence, net field-aligned currents are feeding the eastward electrojet west of profile 5 (east of profile 5 J_y is presumably constant).

The magnetic field of the net field-aligned currents feeding the eastward electrojet causes positive level shifts or steps in the latitude profiles of the east-west component observed on the ground (Hughes and Rostoker, 1977, 1979; Baumjohann et al. 1980; Baumjohann and Kamide, 1981). The positive level shifts can easily be recognized in the measured B_M profiles given in Figure 3. Despite the poor station coverage in the region of westward Hall currents a negative level shift can be seen north of the eastward electrojet. This negative level shift may indicate that part of the substorm-associated westward electrojet diverges up the magnetic field lines. However, these upward net field-aligned currents are weaker than those downward directed ones over the eastward electrojet (since the positive B step is larger than the negative B step) and thus the SMA magnetometers indicate downward overall net field-aligned currents which is an apparent contradiction to the TRIAD measurements.

However, the apparent inconsistency which has also been noted by Hughes and Rostoker (1979) and Baumjohann et al. (1980) can be resolved since it is not so much a physical problem but is more a matter of interpretation related to different definitions of the term "net field-aligned current". Ground-based magnetometers mainly respond to those field-aligned currents which are closing longitudinally via the electrojets and thus ground-based magnetometer people define these field-aligned currents as net field-aligned currents (in accord with the original definition by Heppner et al. 1971a, b which will also be used throughout the present paper) while TRIAD experimenters define net field-aligned currents as those currents which are not balanced along one meridional cross section of the auroral oval. As already suggested by Hughes and Rostoker (1979) the latter may incorporate also field-aligned currents which close meridionally via polar cap currents and which are observed by satellites but cannot be detected by magnetometers on the ground.

We will show that in our case a part of the upward field-aligned current observed by TRIAD is closed meridionally via the polar cap by duskward Pedersen currents and downward field-aligned currents in the dawn sector of the auroral oval (downward field-aligned currents north of the dawn sector westward electrojet have actually been found by Kamide et al., 1976). Moreover, we will also show that a part of the inconsistency

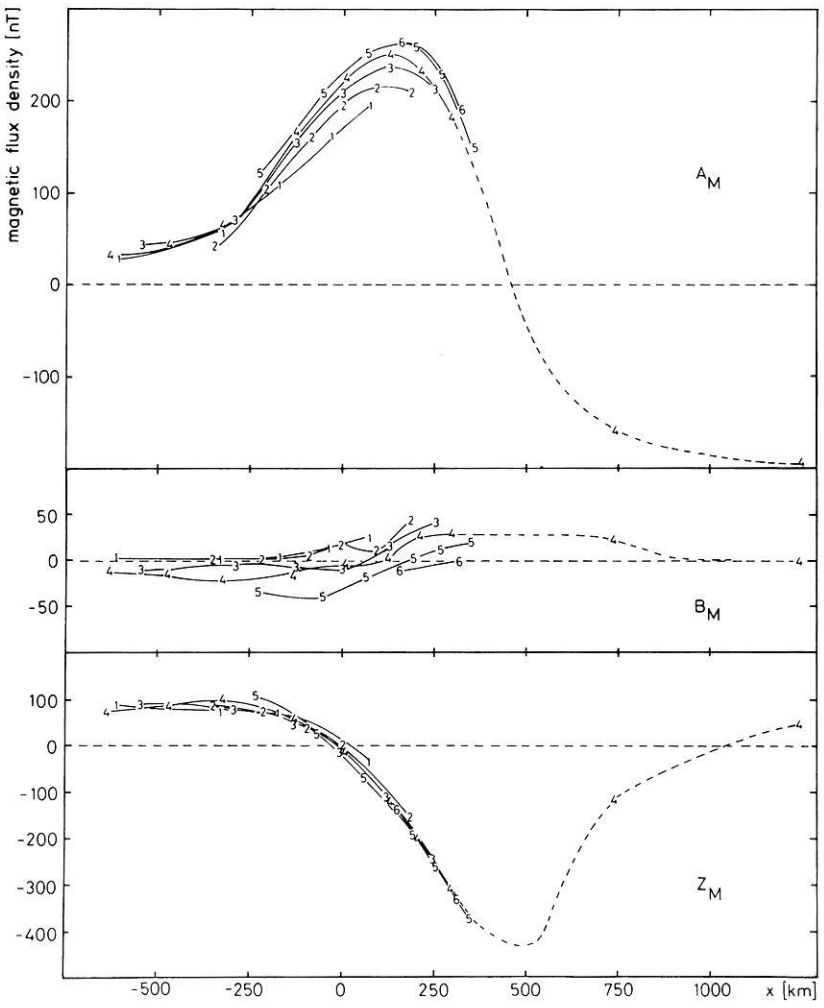

Fig. 3. Latitude profiles of the 4 min averaged A_M (parallel x), B_M (parallel y) and Z_M (vertical) components measured on the ground. The numbers denote the different profiles (1 to 6 from west to east) and simultaneously give the location of and the amplitude observed at the respective station

stems from the fact that the field-aligned current sheets have different finite east-west extents and that the sheet current densities of the shorter current sheets, in particular, may be severely underestimated when using the conventional infinite current sheet formulas.

Numerical Modelling

From the analysis above it becomes clear that it is possible to deduce the essential components of the current system (eastward electrojet, westward electrojet, polar cap currents, net up- and downward field-aligned currents etc.) causing the aforementioned magnetic disturbances directly from the latitude profiles displayed in Figure 2 and 3. Moreover, it is even possible to infer some first estimates on the boundaries and longitudinal and latitudinal current density distributions. In order to confirm this semi-quantitative analysis and to determine final values for electrojet boundary positions and current density distributions we have set up the model current system displayed in Figure 4 based on our analysis above and have fitted it to our data in the manner described below.

The Model

The upper panel of Figure 4 shows the meridional part of the total model current system, which consists of the following components: (1) the duskward Pedersen currents flowing in the polar cap and in the region of the substorm intensified westward electrojet, (2) the northward Pedersen currents over the eastward electrojet, and (3) the associated balanced field-aligned currents. As can be seen the polar cap has been approximated by a rectangle which, of course, is a crude approximation of the real geometry but good enough to reproduce the effects of the polar cap currents in the Scandinavian area. While the polar cap Pedersen current density is presumably uniform (and thus the associated balanced field-aligned currents are also uniform in intensity) the sheet current density of the meridional current system over the eastward electrojet increases concurrently with the eastward electrojet itself between $y=-1{,}700$ km to $y=300$ km (profile 5) and stays constant until $y=3{,}300$ km. The latter assumption is equivalent to a longitudinally constant Hall-to-Pedersen conductivity ratio in the eastward electrojet region and is in agreement with the results of Brekke et al. (1974). We should note that our model calculations cannot confirm a strict longitudinal constancy of the conductivity ratio. However, we can rule out that the meridional current system stays constant with latitude since this would lead to unrealisticly small Hall-to-Pedersen conductivity ratios west of Scandinavia

The downward net field-aligned current that feeds the eastward electrojet between $y=-1{,}700$ km and $y=300$ km is shown in the lower panel of Figure 4 together with the eastward electrojet whose current strength increases linearly in the same region. In the polar cap a broad sunward Hall current flows and along the northern border of the auroral oval a substorm-intensified westward electrojet penetrates into the dusk sector (in the region of southward Pedersen currents) and diverges up magnetic field lines. South of the eastward electrojet, in subauroral latitudes,

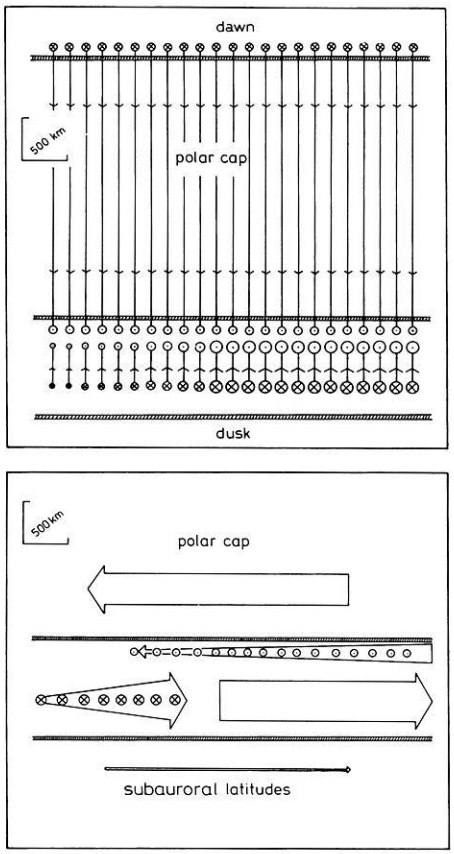

Fig. 4. Sketch of the model current system. The *upper diagram* gives the field-aligned currents in the dusk sector auroral zone and at the dawn sector polar cap boundary which close meridionally via Pedersen currents in the dusk sector auroral zone and in the polar cap. The *lower panel* shows the Hall currents in the dusk sector auroral zone, at subauroral latitudes and in the polar cap and their associated net field-aligned currents. *Circles* with dots indicate upward field-aligned currents while circles with crosses show downward flowing currents. The size of the circles and of the arrowheads and the thickness of the arrows approximately gives the current densities of the field-aligned, Pedersen and Hall currents, respectively. The hatched horizontal bars denote equatorward and poleward boundaries of the auroral zone

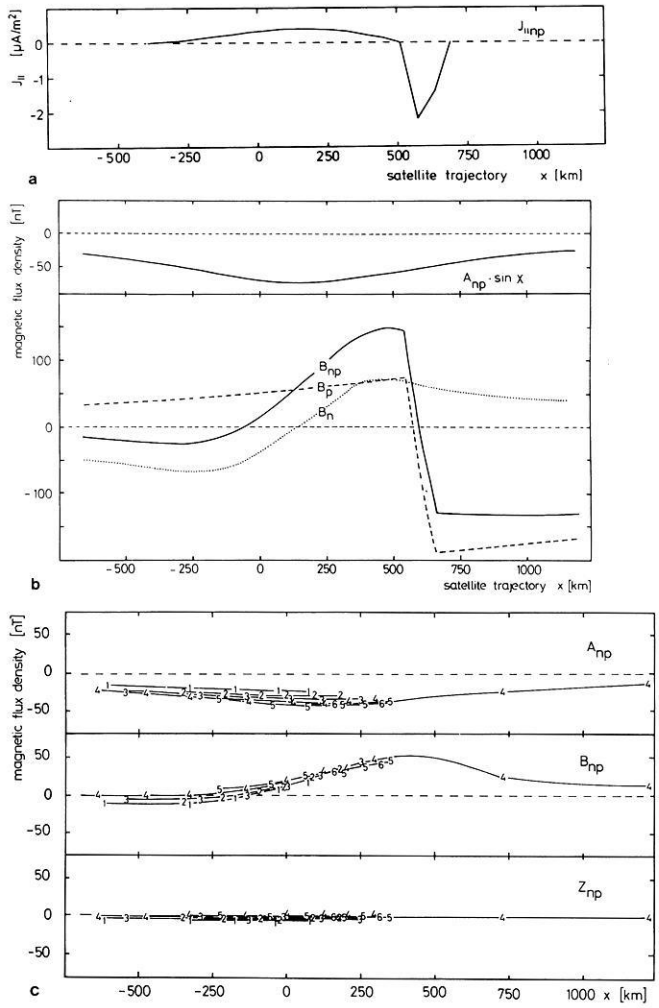

Fig. 5. a Model current density distribution along the TRIAD track of the net field-aligned currents feeding the eastward electrojet and diverging from the westward electrojet and from the polar cap Pedersen currents. **b** Horizontal magnetic components along the satellite track. B_n is caused by the net field-aligned currents feeding the eastward electrojet. B_p is caused by the net field-aligned currents diverging from the westward electrojet and the meridional polar cap current system. B_{np} is the sum of B_n and B_p and $A_{np} \cdot \sin\chi$ is the respective north-south component (χ denotes the inclination of the field lines). **c** Magnetic field perturbations measured on the ground. The same notations are used as in **b**

flows a comparatively very weak UV electrojet (see Rostoker et al., 1979). No (possibly existing) meridional currents in the UV electrojet region have been included in our model current system. Not shown in the figure but included in the model is a downward net field-aligned current sheet (of the same sheet current density as the upward net field aligned current over the westward electrojet) at the northern border of the dawn sector auroral oval. Such currents have been reported by, for example, Iijima and Potemra (1976), Sugiura and Potemra (1976), McDiarmid et al. (1978, 1979) and Hughes and Rostoker (1979).

In order to calculate the magnetic fields caused by the model currents at the ground and along the TRIAD trajectory we have divided the ionosphere in small cells of $\Delta y = 50$ km and $\Delta x = 60$ km each and approximated the current density distribution by vertical and horizontal line currents whose current strength is constant within a single cell. Since the geometry of the spherical earth is somewhat distorted by the transformation into the Kiruna system at great distances from Kiruna especially in the polar cap, any absolute values given for x or y greater than, say, 1,500 km should be regarded more qualitatively than quantitatively.

For a non-homogeneous conductivity distribution the magnetic field on the ground will be severely influenced by the presence of the net field-aligned currents (Baumjohann et al., 1980). Therefore we first derived the net and balanced field-aligned and Pedersen current densities by fitting the calculated B_T (at satellite altitude) and B_M (on the ground) components to the corresponding observed components (these are not influenced by the east-west Hall currents). After subtraction of the calculated A_M and Z_M components due to the same currents from the observed components, the heightintegrated eastward and westward Hall current densities in the ionosphere have been calculated from the residual components by field separation and upward continuation as described by Baumjohann et al. (1979) and Sulzbacher et al. (1980).

Hence, in the following we will first give parameters of net

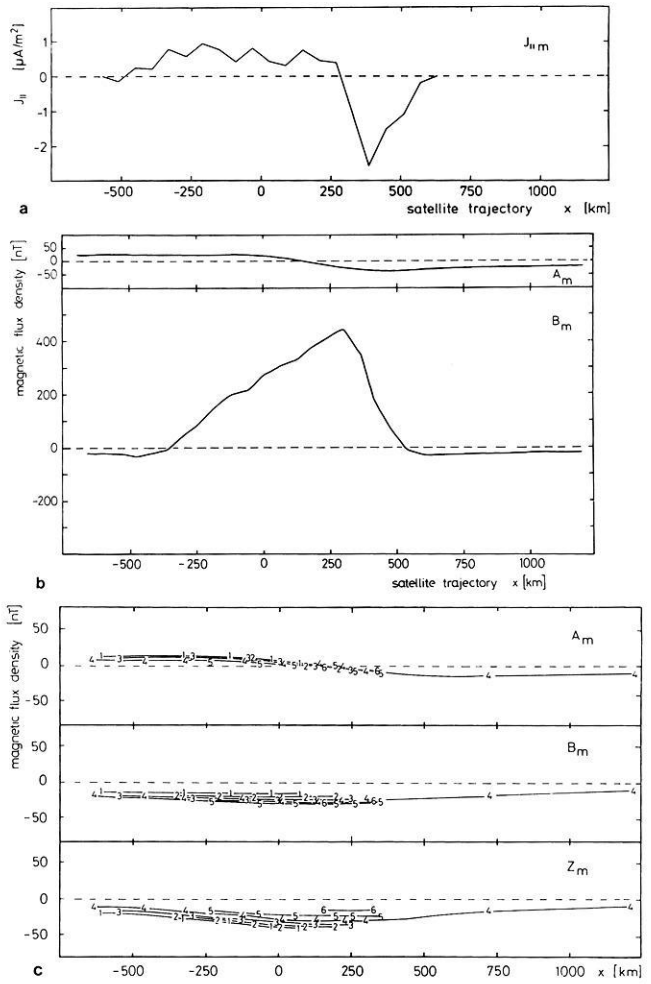

Fig. 6. a Model current density distribution along the TRIAD track of the balanced field-aligned currents closed by northward Pedersen currents in the auroral zone. **b** Horizontal magnetic components along the satellite track caused by the meridional current system in the auroral zone. **c** Magnetic components on the ground. The same notations are used as in **b**

field-aligned currents and polar cap currents and their associated magnetic fields on the ground and at TRIAD's altitude (projected down along magnetic field lines to ionospheric heights), then those of the meridional current system in the auroral zone and finally compare ionospheric Hall and Pedersen currents. Afterwards we will compare calculated and measured fields due to the total current system, include electric field data and derive conductivities.

Net Field-Aligned and Polar Cap Currents

The resultant distribution along the TRIAD trajecory of those field-aligned currents that close either longitudinally via Hall currents in the auroral zone or meridionally via polar cap Pedersen currents is displayed in Fig. 5a. The magnetic field components generated by these currents and the dawn-to-dusk polar cap Pedersen currents along the TRIAD trajectory and at the SMA stations are shown in Figure 5b and 5c, respectively.

The field-aligned current sheet that feeds the eastward electrojet extends about 2,000 km in longitude and has a sheet current density of about 220 mAm^{-1} and a maximum current density of 0.4 μAm^{-2}. North of this rather broad region of downward net field-aligned currents exists a latitudinally more confined but longitudinally more extended (about 5,000 km) region of intense upward field-aligned current (up to 2.2 μAm^{-2}). About 60% of these upward field-aligned currents (125 mAm^{-1}) are closed via the polar cap while 40% (95 mAm^{-1}) originate from the longitudinal divergence of the westward electrojet.

Hence, between $y=-1{,}700$ km and $y=+300$ km the downward net field-aligned currents feeding the eastward electrojet have the same sheet current intensity as the upward field-aligned currents to the north and it is only east of $y=+300$ km (where the longitudinal divergence of the eastward electrojet is zero) that more field-aligned current flows upward than downward.

Figure 5b, where we have displayed the magnetic effects of the downward net field-aligned currents and of the upward net field-aligned currents and the meridional polar cap current system at TRIAD's altitude separately (B_n and B_p, respectively), shows clearly that the finite extent of the field-aligned current sheets has to be included, particularly to reproduce the TRIAD observations: if the east-west extent of the downward field-aligned current sheet were not much smaller than that of the upward field-aligned current sheet (2,000 km viz. 5,000 km), the level shifts of the equally strong downward and upward field-aligned current sheets would just cancel each other. The A components observed at TRIAD and on the ground are mainly caused by edge effects of the downward net field-aligned current sheet.

The Meridional Auroral Current System

As stated above, we have assumed that the Σ_H/Σ_P ratio is longitudinally constant in the eastward electrojet region and thus the Pedersen and balanced field-aligned current density in the dusk sector of the auroral zone is supposed to grow linearly between $y=-1{,}700$ km and $y=+300$ km with the eastward electrojet and to stay constant east of $y=+300$ km.

In Figure 6a the balanced field-aligned current density is displayed along the satellite trajectory. Again, the downward field-aligned currents are more broadly distributed (over about 800 km) but less intense (0.4–0.8 μAm^{-2}) than the upward field-aligned currents to the north (300 km and up to 2.3 μAm^{-2}).

The latitude profile (along the satellite trajectory) of the east-west magnetic field component caused by the meridional auroral zone current system (B_m) is shown in the lower panel of Figure 6b. The maximum amplitude of this nearly toroidal magnetic field amounts to about 440 nT. Since the current density of the meridional current system increases to the east, some magnetic flux leaks out and can be seen in the slightly negative B_m components north and south of the meridional current system and especially in the north-south A_m components (upper panel of Fig. 6b) which show a positive deflection of about 30 nT in the south and a negative one of about 35 nT north of the B_m maximum.

The leakage of magnetic flux out of the meridional current system can also be seen on the ground (Fig. 6c). Here the A_m component amounts to about 30%–60% of that seen at satellite altitude and the 'leakage' B_m component has about 60% of its magnitude calculated for the TRIAD trajectory. The Z_m components (lower panel of Fig. 6c) stem from gradients of the ionospheric Pedersen currents.

Height-Integrated Ionospheric Hall and Pedersen Currents

The height-integrated Hall current density J_H and Pedersen current density J_P along the satellite trajectory ($y=125$ km) are displayed in Figure 7. The Hall current density was calculated by field separation and upward continuation of the measured

A_M and Z_M components to 120 km altitude (average height of eastward electrojet after Kamide and Brekke, 1977) after the aforementioned A_{np}, A_m, Z_{np} and Z_m had been subtracted. At $y=300$ km, where the eastward electrojet has its maximum, the maximum Hall current density amounts to about 800 mAm^{-1} and the total Hall current to $4.15 \cdot 10^5$ A. The height-integrated Pedersen current density reached a maximum value of 420 mAm^{-1}. The total Hall current strength increases by 210 mAm^{-1} when going to the east as compared to the independently calculated downward net field-aligned sheet current density of 220 mAm^{-1} and thus current continuity after Eq. (2) also holds quantitatively. The difference in the reversal of the direction of Hall and Pedersen currents is mainly due to the poor data coverage on the ground north of the Scandinavian coastline and thus to some uncertainty in the Hall current density distribution north of $x=300$ km. Part of this difference may also be due to uncertainties in the calculation of the TRIAD magnetic field baseline.

South of the eastward electrojet the so-called UV electrojet can be recognized. It is very weak and has a height-integrated Hall current density of less than 40 mAm^{-1}. North of the eastward electrojet a small region of enhanced westward Hall current (about 600 mAm^{-1}) can be seen which may be identified as the substorm-associated westward electrojet. Note that there is no enhancement of the Pedersen current in that region. Within the polar cap a Hall current with a height-integrated current density of about 300 mAm^{-1} is flowing, compared to the aforementioned dawn-to-dusk Pedersen current of 125 mAm^{-1}.

Comparison of Calculated and Measured Magnetic Fields Due to the Total Current System

All measured magnetic field and equivalent current vectors at TRIAD and on the ground, respectively, are shown in Figure 8 by dashed arrows, while the values calculated from our best-fit model are indicated by solid arrows. It can be seen that there is a very good fit of the equivalent current vectors measured and calculated on the ground and also a good fit of the measured and calculated east-west B_T components along the satellite track, but the measured A_T component is not reproduced so well.

In particular, the calculated B_T is the sum of B_n, B_p and B_m shown in Figures 5b and 6b and reproduces the measured B_T nearly exactly if one adds a uniform field of 40 nT which can be ascribed to uncertainties in the base line reduction scheme (Gustafsson et al., 1981). The calculated A_T at TRIAD altitude results mainly from the edge of the downward net field-aligned current (A_{np}, Fig. 5b), from the leakage of the nearly toroidal magnetic field within the meridional current circuit (A_m, Fig. 6b) and from the field of the ionospheric Hall current at TRIAD altitude (not shown here, but see Sulzbacher et al., 1980, for a more complete analysis of this contribution). Even if a uniform field of -100 nT (due to base line uncertainties) is added to A_T, a clearly visible difference remains. This difference has probably mainly to be attributed to an enhancement of upward field-aligned currents in the region of the terminator ($x=300$–600 km) that are not included in the model but have been observed earlier by, for example, Hughes and Rostoker (1979).

On the ground, the calculated A_M component is mainly due to the Hall currents and includes the A_{np} (Fig. 5c) and A_m (Fig. 6c) contributions. The calculated B_M components are composed of the above discussed B_{np} (Fig. 5c) and B_m (Fig. 6c). They fit the measured B_M components if a longitude-dependent but latitudinally uniform field is added that decreases from west (about $+15$ nT) to east (about -15 nT). The cause of this field contribution is as yet unclear. The Z_M components on the ground

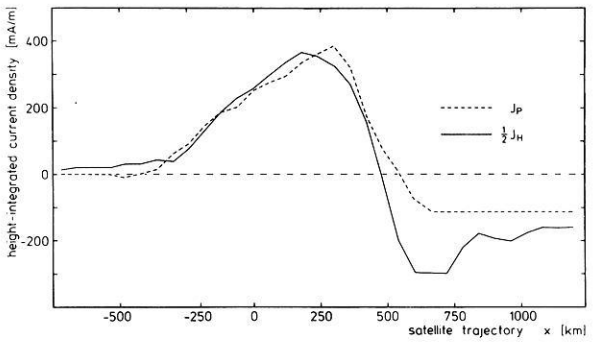

Fig. 7. Calculated Hall and Pedersen current densities of the model current system along the TRIAD trajectory

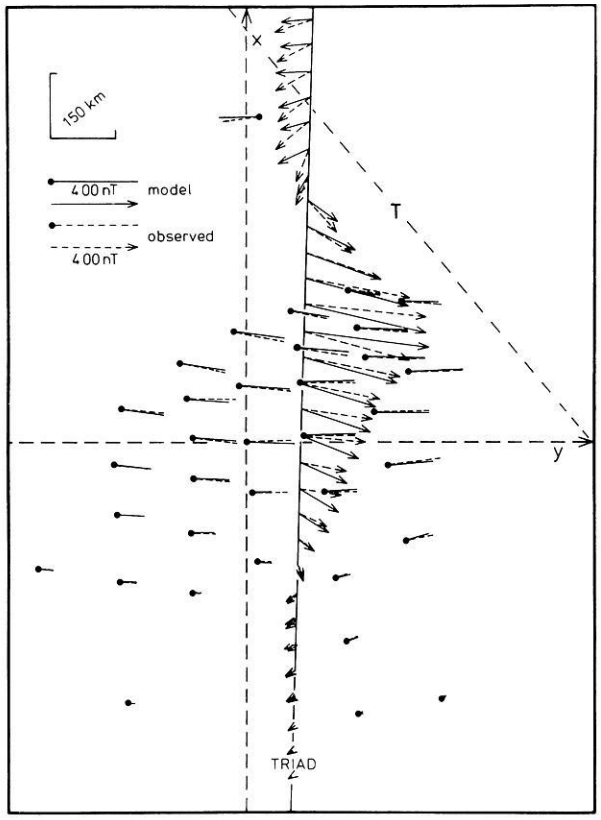

Fig. 8. Observed (dashed) and modelled (solid) equivalent current and magnetic disturbance vectors on the ground and along the TRIAD trajectory. Otherwise same as Fig. 1

are mainly caused by the Hall currents, but are also influenced by the longitudinal gradients of the meridional current system (Z_m, Fig. 6c). The east-west gradients in the Z_m components partly balance those caused by the eastward electrojet and are thus the cause for the comparatively weak east-west gradients in the measured Z_m components (Fig. 3).

Electric Field and Height-Integrated Conductivities

In Figure 9 we display contours of the electric field derived from the Trondheim radar measurements under the assumption that the electric field is parallel to the x axis (see above). It can be seen that the electric field amplitude increases nearly linearly from south to north and also, but more weakly, from east to west.

The two-dimensional distribution of the height-integrated

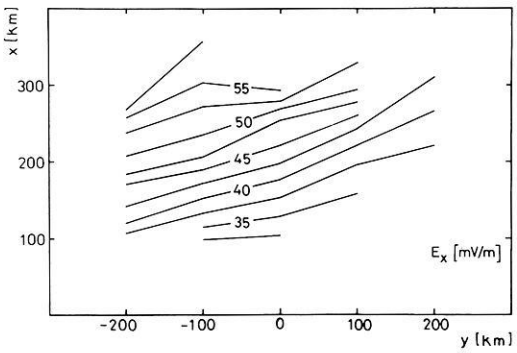

Fig. 9. Contours of the northward ionospheric electric field calculated from the Trondheim radar observations under the assumption that the electric field is directed parallel to the x axis

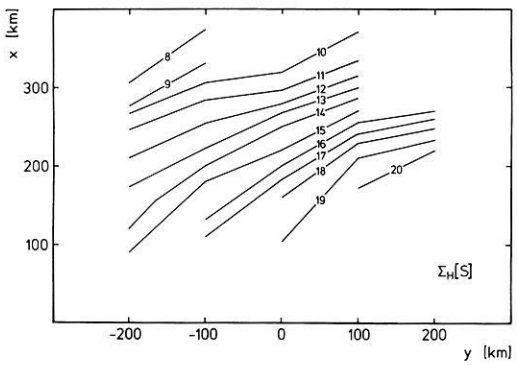

Fig. 10. Contours of the Hall conductivity distribution

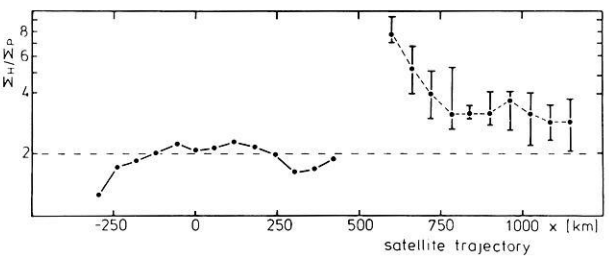

Fig. 11. Hall-to-Pedersen conductivity ratio along the TRIAD trajectory. The error bars give the estimated uncertainty that is caused by the poor data coverage in that region

Hall conductivity is easily calculated from the electric field values and the Hall current density derived from the two-dimensional SMA observations. Σ_H is shown in Figure 10 and ranges from 8–20 S. Σ_H decreases linearly to the north and increases to the east. Both features, i.e. latitudinal anticorrelation between Hall conductivity and electric field and increase of Hall conductivity to the east, have also been observed by Baumjohann et al. (1980) in the same MLT sector. It should be noted that Scandinavia is still slightly west of the terminator (cf. Fig. 1) and that the solar-UV generated conductivity may play a role in the eastward electrojet region. However, the increase of the Hall conductivity to the east is clearly anticorrelated to the solar zenith angle and must be due to increasing particle precipitation closer to magnetic midnight.

Since the Pedersen current density is calculated on the base of the latitudinal TRIAD measurements and the two-dimensional distribution of J_P in our model was based on the assumption of an east-west uniform Σ_H/Σ_P ratio, it is of no use to give a two-dimensional Σ_P distribution. However, Σ_P may be calculated along that part of the satellite trajectory that lies within the STARE observation area. Here Σ_p decreases nearly linearly from about 10 S in the south to 5 S in the north.

The Hall to Pedersen conductivity ratio can be calculated along the whole satellite trajectory even north of the STARE observation area, since this calculation involves only J_H and J_P. The result is shown in Figure 11 and it can be seen that Σ_H/Σ_P is about 2 in the eastward electrojet region while it increases up to 8 within the substorm-associated westward electrojet and decreases to values around 3 in the polar cap. No values can be given for the region where J_H and J_P reverse their direction. The error bars in the northern part of the Σ_H/Σ_P ratio profile stem from uncertainties in the interpolation of the magnetic field latitude profiles between the two northernmost observatories and the stations on the Scandinavian mainland.

Discussion

In the following we will discuss some aspects of the coupling between large-scale field-aligned currents and ionospheric currents in the dawn-dusk sector, which are not yet fully understood (Hughes and Rostoker, 1979). For the analysed event on 4 January 1979 we have provided quantitative values for main ionospheric and field-aligned currents. The calculated values for fields, currents and conductivities are within the range of other values derived from satellite and radar measurements. Moreover, it is possible to draw conclusions on the energy of precipitating particles in the dusk sector from the calculated Σ_H/Σ_P ratios.

The Large-Scale Three-Dimensional Current System in the Dusk Sector

The model calculations strongly support our statement above that the inconsistency between downward net field-aligned current determined from ground-based magnetometers and upward net field-aligned current seen by satellite magnetometers in the afternoon sector is an apparent one and can be resolved by taking the polar cap currents and the different finite extent of the field-aligned current sheets into account. Figure 12, where we show B_M and B_T profiles calculated for our model current system between $y=-1{,}700$ km and $y=+800$ km (about 13–19 MLT) every 500 km (about 1 h local time), shows this even more clearly: Between $y=-1{,}700$ km and $y=300$ km the ground-based B_M profiles (left panel) show positive and negative level shifts mainly due to the downward net field-aligned current feeding the eastward electrojet and the comparatively weaker upward net field-aligned current diverging from the substorm associated westward electrojet, respectively. More easterly, i.e. at $y=800$ km (about 18–19 MLT), only edge effects of the downward net field-aligned current sheet can be seen, but they still have about the same magnitude as the disturbance caused by the weaker upward net field-aligned currents. The B_T profiles (right panel) show, throughout the whole longitudinal range, negative level shifts, which are substantially caused by the meridional polar cap current system with its long east-west extent and its nearly toroidal field. In the conventional infinite current sheet interpretation those would be ascribed to upward net field-aligned currents, but it is only at $y \geqq 300$ km where more field-aligned current flows upward than downward.

Moreover, Figure 12 shows that our results are in qualitative agreement with more statistical observations by Hughes and Rostoker (1979), who give average B_M profiles, and the ISIS-2 measurements by McDiarmid et al. (1978, 1979), whose dusk sector auroral oval and especially polar cap B_T measurements fit quite well to our model profiles. The measurements of

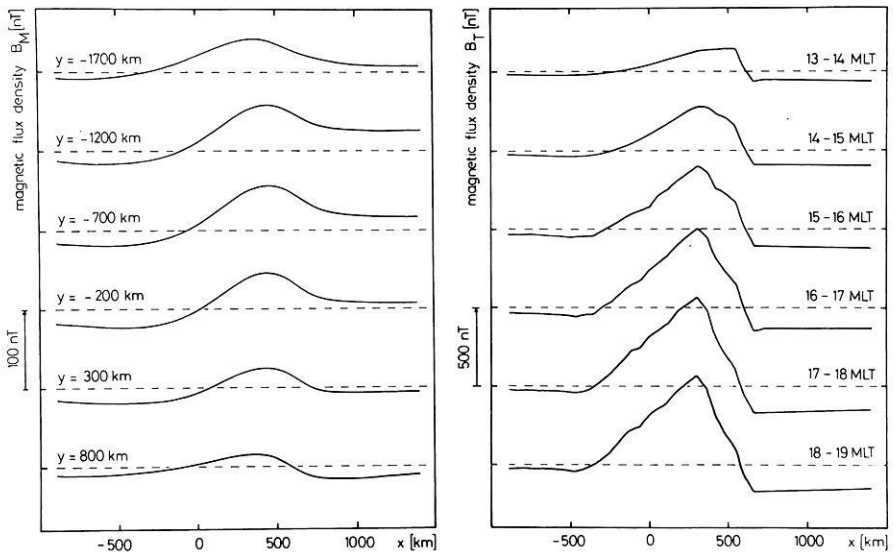

Fig. 12. Latitude profiles of the calculated B_M (*left diagram*) and B_T (*right diagram*) components in the afternoon and early evening sector, each separated by $\Delta y = 500$ km (about 1 h MLT). The *dashed lines* give the zero levels

McDiarmid et al. (1978, 1979) fit nearly exactly if one assumes that our observations were made during a period when the IMF B_z component was negative and B_y was close to zero. However, a wide range of IMF orientations can easily be reproduced simples by changing the current densities in our model.

Hence, our results suggest that, in contradiction to earlier analyses of either purely ground-based or purely satellite magnetic data (e.g. Sugiura and Potemra, 1976; Iijima and Potemra, 1976, 1978; Hughes and Rostoker, 1977, 1979), during *active* times no more field-aligned current may flow in than out of the afternoon sector of the auroral oval. This is consistent with an earlier proposal made by Heppner in 1971a, b. However, it may well be that during *quiet* times, when eastward and westward electrojets and the associated net field-aligned currents are very weak, the polar cap current system may still persist and thus significant field-aligned currents may flow out of the ionosphere along the northern border of the afternoon auroral oval.

Σ_H/Σ_P Ratio and Latitudinal Morphology of Precipitating Particles

The Σ_H/Σ_P ratio shown in Figure 11 is within the range of values found by other observational methods such as the Chatanika radar (Brekke et al., 1974; Horwitz et al., 1978 a, b; Vickrey et al., 1981); rocket-borne measurements (Evans et al., 1977; Behm et al., 1979; Cahill et al., 1980; Brüning et al., 1981; Theile et al., 1981) and satellite detectors (Wallis and Budzinski, 1981) in the afternoon and evening sector of the auroral oval. This is expecially gratifying since our method (see also Baumjohann et al., 1979, and Sulzbacher et al., 1980) is quite different from the methods given above: our method involves only magnetic field measurements but no neutral atmosphere model as all the others do.

According to the results of Rees (1963) and, for example, Vondrak and Baron (1977) and Vondrak and Sears (1978), conclusions about the energy of the precipitating particles can be drawn from the Σ_H/Σ_P ratio (see also Sulzbacher et al., 1980). From the relatively small Σ_H/Σ_P ratio between $x = -500$ km and $x = -250$ km we may conclude that the energy of particles precipitating in this region is rather small, while the increasing ratio in the central and northern part of the eastward electrojet indicates a hardening of the precipitating particle population. The comparatively high Σ_H/Σ_P ratio in the westward electrojet region gives an additional hint that this current is associated with a substorm, i.e. caused by the injection and precipitation of high-energy particles during the substorm.

It is somewhat astonishing that the Σ_H/Σ_P ratio is greater in the polar cap than in the eastward electrojet region. This means that the particle population precipitating in the diffuse aurora and originating from the central plasma sheet (cps; Winningham et al., 1975; Lui et al., 1977) must be less energetic than that precipitating in the polar cap. However, usually the polar rain is less energetic (around 100 eV) than the cps precipitation (around 1 keV) and we may thus conclude that during the present event the polar cap conductivity was created by the substorm-associated polar squall (Winningham and Heikkila, 1974) which can include electrons with energies higher than 1 keV.

Conclusions

In the present study we were able to fit a three-dimensional modell current system to simultaneous SMA and TRIAD observations of magnetic disturbances in the dusk sector. Accordingly it was possible to determine quantitatively the parameters of the main current loops and to get relevant information on the coupling between ionospheric and field-aligned currents in the dusk and also partially in the dawn sector. We have presented evidence that our model current system is at least qualitatively representative of the magnetic observations obtained by ISIS-2, TRIAD and the Alberta magnetometer chain and that it can resolve an apparent contradiction that resulted from ambiguities when interpreting either groundbased or satellite magnetic measurements alone. Calculation of the Σ_H/Σ_P ratio along the TRIAD trajectory from magnetic measurements alone enabled us to draw conclusions about the energy of precipitating particles along that meridian and by including measurements of the STARE Trondheim radar and assuming that the ionospheric electric field was aligned perpendicular to the eastward electrojet we could calculate the two-dimensional distribution of the Hall conductivity within the STARE observation area.

In our opinion, the result most relevant to the physics of current systems in and above the auroral zone is that during times of high magnetospheric activity, as in the present case, inward and outward field-aligned currents tend to be totally balanced in the afternoon sector but that there are different

ways to close these currents meridionally (by auroral zone and polar cap Pedersen currents) and longitudinally (via Hall currents). The distinction between the field-aligned currents closing via Pedersen and those closing via Hall currents is particularly important, since it is very likely that they have different sources: Pedersen currents dissipate energy through Joule heating and thus the field-aligned currents feeding them must be driven by a magnetospheric generator (Rostoker and Boström, 1976) while the Hall currents do not involve energy dissipation and the source of the field-aligned currents feeding and closing them does not require input and may be either constituted by the vorticity of the magnetospheric plasma drift (Rostoker, 1979) or by longitudinal gradients in the ionospheric conductivity (Akasofu et al., 1981).

Acknowledgements. We are greatly indebted to the past and present members of the magnetometer group at the University of Münster. We especially thank B. Inhester, D. Schmidt and J. Untiedt for numerous fruitful discussions. The magnetic observations were performed in cooperation with the Royal Institute of Technology at Stockholm, the Finnish Meteorological Institute at Helsinki, the University of Tromsö, the University of Bergen, the Geophysical Observatory at Sodankylä, the Kiruna Geophysical Institute, the University of Oulu, and the Aarhus University. To these institutions our sincere thanks are due for permanent support. Invaluable assistance in the TRIAD data collection and processing was provided by S. Favin, J. DuBrul, and J. Neary, and the entire project was made possible by the Space Department of APL/JHU. We also thank the Kiruna Geophysical Institute for assistance in the acquisition of the Triad data. The Trondheim radar measurements are made in cooperation with ELAB and the Technical University at Trondheim. Finally we would like to thank H. Maurer (TU Braunschweig) and St. Berger (University of Tromsö) who made additional magnetic data available to us. This work has been supported financially by the Deutsche Forschungsgemeinschaft, the National Science Foundation, and the Office of Naval Research.

References

Akasofu, S.-I., Kamide, Y., Kan, J.R., Lee, L.C., Ahn, B.-H.: Power transmission from the solar wind – magnetosphere dynamo to the magnetosphere and to the ionosphere: Analysis of the IMS Alaska meridian chain data. Planet. Space Sci. **29**, 721–730, 1981

Anderson, H.R., Vondrak, R.R.: Observations of Birkeland currents at auroral latitudes. Rev. Geophys. Space Phys. **13**, 243–262, 1975

Armstrong, J.C., Zmuda, A.J.: Triaxial magnetic measurements of field-aligned currents at 800 kilometers in the auroral region: initial results. J. Geophys. Res. **78**, 6802–6807, 1973

Banks, P.M., Doupnik, J.R.: A review of auroral zone electrodynamics deduced from incoherent scatter radar observations. J. Atmos. Terr. Phys. **37**, 951–972, 1975

Banks, P.M., Doupnik, J.R., Akasofu, S.-I.: Electric field observations by incoherent scatter radar in the auroral zone. J. Geophys. Res. **78**, 6607–6622, 1973

Baumjohann, W.: Spatially inhomogeneous current configurations as seen by the Scandinavian Magnetometer Array. In: Proceeding of the International Workshop on Selected Topics of Magnetospheric Physics, Japanese IMS Committee, eds., pp. 35–40. Tokyo 1979

Baumjohann, W., Kamide, K.: Joint two-dimensional observations of ground magnetic and ionospheric electric fields associated with auroral zone currents. 2. Three-dimensional current flow in the morning sector during substorm recovery. J. Geomagn. Geoelectr. **33**, 297–318, 1981

Baumjohann, W., Greenwald, R.A., Küppers, F.: Joint magnetometer array and radar backscatter observations of auroral currents in Northern Scandinavia. J. Geophys. **44**, 373–383, 1978

Baumjohann, W., Sulzbacher, H., Potemra, T.A.: Joint magnetic observations of small-scale structures in a westward electrojet with Triad and the Scandinavian Magnetometer Array. In: Proceeding of the International Workshop on Selected Topics of Magnetospheric Physics, Japanese IMS committee, eds, pp 49–52. Tokyo 1979

Baumjohann, W., Untiedt, J., Greenwald, R.A.: Joint two-dimensional observations of ground magnetic and ionospheric electric fields associated with auroral zone currents 1. Three-dimensional current flows associated with a substorm-intensified eastward electrojet. J. Geophys. Res. **85**, 1963–1978, 1980

Behm, D.A., Primdahl, F., Zanetti, L.J., Jr., Arnoldy, R.L., Cahill, L.J., Jr.: Ionospheric electrical currents in the late evening plasma flow reversal. J. Geophys. Res. **84**, 5339–5343, 1979

Boström, R.: A model of the auroral electrojets. J. Geophys. Res. **69**, 4983–5000, 1964

Brekke, A., Doupnik, J.R., Banks, P.M.: Incoherent scatter measurements of E region conductivities and currents in the auroral zone. J. Geophys. Res. **79**, 3773–3790, 1974

Brüning, K., Baumjohann, W., Wilhelm, K., Stüdemann, W., Urban, A., Ott, W., Spenner, K., Schmidtke, G.L., Fischer, H.M.: On different methods of calculating conductivities of the auroral ionosphere from sounding rocket observations. J. Geophys. **49**, 74–81, 1981

Cahill, L.J. Jr., Arnoldy, R.L., Taylor, W.W.L.: Rocket observations at the northern edge of the eastward electrojet. J. Geophys. Res. **85**, 3407–3413, 1980

Evans, D.S., Maynard, N.C., Trøim, J., Jacobsen, T., Egeland, A.: Auroral vector electric fields and particle comparisons. 2. Electrodynamics of an arc. J. Geophys. Res. **82**, 2235–2249, 1977

Friis-Christensen, E., Wilhjelm, J.: Polar cap currents for different directions of the interplanetary magnetic field in the Y-Z plane. J. Geophys. Res. **80**, 1248–1260, 1975

Greenwald, R.A.: Studies of currents and electric fields in the auroral zone ionosphere using radar auroral backscatter. In: Dynamics of the magnetosphere, S.-I. Akasofu, ed., pp. 213–248. Dordrecht: D. Reidel 1979

Greenwald, R.A., Weiss, W., Nielsen, E., Thomson, N.R.: STARE: a new radar auroral backscatter experiment in northern Scandinavia. Radio Sci. **13**, 1021–1039, 1978

Gustafsson, G.: A revised corrected geomagnetic coordinate system. Ark. Geofys. **5**, 595–617, 1970

Gustafsson, G., Potemra, T.A., Favin, S., Saflekos, N.A.: Distant magnetic field effects associated with Birkeland currents (made possible by the evaluation of Triad's attitude oscillations). J. Geophys. Res. **86**, 9219–9223, 1981

Heelis, R.A., Hanson, W.B.: High-latitude ion convection in the nighttime F region. J. Geophys. Res. **85**, 1995–2002, 1980

Heppner, J.P.: Electric field variations during substorms: OGO-6 measurements. Planet. Space Sci. **20**, 1475–1498, 1972

Heppner, J.P.: High latitude electric fields and the modulations related to interplanetary magnetic field parameters. Radio Sci. **8**, 933–948, 1973

Heppner, J.P.: Empirical models of high-latitude electric fields. J. Geophys. Res. **82**, 1115–1125, 1977

Heppner, J.P., Stolarik, J.D., Wescott, E.M.: Electric field measurements and the identification of currents causing magnetic disturbances in the polar cap. J. Geophys. Res. **76**, 6028–6053, 1971a

Heppner, J.P., Stolarik, J.D., Wescott, E.M.: Field-aligned continuity of Hall current electrojets and other consequences of density gradients in the auroral ionosphere. In: The radiating atmosphere, B.M. McCormac, ed., pp. 407–426. Dordrecht: D. Reidel 1971b

Holzworth, R.H., Berthelier, J.-J., Cullers, D.K., Fahleson, U.V., Fälthammar, C.-G., Hudson, M.K., Jalonen, L., Kelley, M.C., Kellogg, P.J., Tanskanen, P., Temerin, M., Mozer, F.S.: The large-scale ionospheric electric field: its variation with magnetic activity and relation to terrestrial kilometric radiation. J. Geophys. Res. **82**, 2735–2742, 1977

Horwitz, J.L., Doupnik, J.R., Banks, P.M.: Chatanika radar observations of the latitudinal distributions of auroral zone electric fields, conductivities, and currents. J. Geophys. Res. **83**, 1463–1481, 1978a

Horwitz, J.L., Doupnik, J.R., Banks, P.M., Kamide, Y., Akasofu, S.-I.: The latitudinal distributions of auroral zone electric fields and ground magnetic perturbations and their response to variations

in the interplanetary magnetic field. J. Geophys. Res. **83**, 2071–2084, 1978b

Hughes, T.J.: A comprehensive model of ionospheric-magnetospheric current systems during periods of moderate magnetospheric activity. Ph. D. thesis, University of Alberta, Edmonton, 1978

Hughes, T.J., Rostoker, G.: Current flow in the magnetosphere and ionosphere during periods of moderate activity. J. Geophys. Res. **82**, 2271–2282, 1977

Hughes, T.J., Rostoker, G.: A comprehensive model current system for high-latitude magnetic activity – I. The steady state system. Geophys. J. R. Astron. Soc. **58**, 525–569, 1979

Hughes, T.J., Oldenbourg, D.W., Rostoker, G.: Interpretation of auroral oval equivalent current flow near dusk using inversion techniques. J. Geophys. Res. **84**, 450–456, 1979

Iijima, T., Potemra, T.A.: The amplitude distribution of field-aligned currents at northern high latitudes observed by Triad. J. Geophys. Res. **81**, 2165–2174, 1976

Iijima, T., Potemra, T.A.: Large-scale characteristics of field-aligned currents associated with substorms. J. Geophys. Res. **83**, 599–615, 1978

Kamide, Y., Akasofu, S.-I.: The auroral electrojet and field-aligned current. Planet. Space Sci. **24**, 203–213, 1976

Kamide, Y., Brekke, A.: Altitude of the eastward and westward auroral electrojets. J. Geophys. Res. **82**, 2851–2853, 1977

Kamide, Y., Fukushima, N.: Positive geomagnetic bays in evening high-latitudes and their possible connection with partial ring current. Rep. Ionos. Space Res. Jap. **26**, 79–101, 1972

Kamide, Y., Matsuhita, S.: Simulation studies of ionospheric electric fields and currents in relation to field-aligned currents. 1. Quiet periods. J. Geophys. Res. **84**, 4083–4098, 1979a

Kamide, Y., Matsushita, S.: Simulation studies of ionospheric electric fields and currents in relation to field-aligned currents. 2. Substorms. J. Geophys. Res. **84**, 4099–4115, 1979b

Kamide, Y., Akasofu, S.-I., Rostoker, G.: Field-aligned currents and the auroral electrojet in the morning sector. J. Geophys. Res. **81**, 6141–6147, 1976

Küppers, F., Untiedt, J., Baumjohann, W., Lange, K., Jones, A.G.: A two-dimensional magnetometer array for ground-based observations of auroral zone electric currents during the International Magnetospheric Study (IMS). J. Geophys. **46**, 429–450, 1979

Lui, A.T.Y., Venkatesan, D., Anger, C.D., Akasofu, S.-I., Heikkila, W.J., Winningham, J.D., Burrows, J.R.: Simultaneous observations of particle precipitations and auroral emissions by the Isis 2 satellite in the 19–24 MLT sector. J. Geophys. Res. **82**, 2210–2226, 1977

Madsen, M.M., Iversen, I.B., D'Angelo, N.: Measurements of high-latitude ionospheric electric fields by means of balloon-borne sensors. J. Geophys. Res. **81**, 3821–3824, 1976

Mallinckrodt, A.J., Carlson, C.W.: Relations between transverse electric fields and the field-aligned currents. J. Geophys. Res. **83**, 1426–1432, 1978

Maurer, H., Theile, B.: Parameters of the auroral electrojet from magnetic variations along a meridian. J. Geophys. **44**, 415–426, 1978

Maynard, N.C.: Electric field measurements across the Harang discontinuity. J. Geophys. Res. **79**, 4620–4631, 1974

Maynard, N.C., Evans, D.S., Maehlum, B., Egeland, A.: Auroral vector electric field and particle comparisons. 1. Premidnight convection topology. J. Geophys. Res. **82**, 2227–2234, 1977

McDiarmid, I.B., Burrows, J.R., Wilson, M.D.: Comparison of magnetic field perturbations at high latitudes with charged particles and IMF measurements. J. Geophys. Res. **83**, 681–688, 1978

McDiarmid, I.B., Burrows, J.R., Wilson, M.D.: Large-scale magnetic field perturbations and particle measurements at 1,400 km on the dayside. J. Geophys. Res. **84**, 1431–1441, 1979

Mersmann, U., Baumjohann, W., Küppers, F., Lange, K.: Analysis of an eastward electrojet by means of upward continuation of ground-based magnetometer data. J. Geophys. **45**, 281–298, 1979

Mozer, F.S., Lucht, P.: The average auroral zone electric field. J. Geophys. Res. **79**, 1001–1006, 1974

Nagai, T., Fukushima, N.: Seasonal dependences of geomagnetic variations in the polar region in connection with large-amplitude annual Z-variation at the geomagnetic pole. Planet. Space Sci. **27**, 1513–1522, 1979

Rees, M.H.: Auroral ionization and excitation by incident energetic electrons. Planet. Space Sci. **11**, 1209–1218, 1963

Rostoker, G.: Polar magnetic substorms. Rev. Geophys. Space Phys. **10**, 157–211, 1972

Rostoker, G.: The auroral electrojets. In: Dynamics of the magnetosphere, S.-I. Akasofu, ed., pp. 201–211. Dordrecht: D. Reidel 1979

Rostoker, G., Boström, R.: A mechanism for driving the gross Birkeland current configuration in the auroral oval. J. Geophys. Res. **81**, 235–244, 1976

Rostoker, G., Hughes, T.J.: A comprehensive model current system for high-latitude magnetic activity – II. The substorm component. Geophys. J.R. Astron. Soc. **58**, 571–581, 1979

Rostoker, G., Kisabeth, J.L.: Response of the polar electrojets in the evening sector to polar magnetic substorms. J. Geophys. Res. **78**, 5559–5571, 1973

Rostoker, G., Armstrong, J.C., Zmuda, A.J.: Field-aligned current flow associated with intrusion of the substorm-intensified westward electrojet into the evening sector. J. Geophys. Res. **80**, 3571–3579, 1975

Rostoker, G., Winningham, J.D., Kawasaki, K., Burrows, J.R., Hughes, T.J.: Energetic particle precipitation into the high-latitude ionosphere and the auroral electrojets. 2. Eastward electrojet and field-aligned current flow at dusk meridian. J. Geophys. Res. **84**, 2006–2018, 1979

Sugiura, M., Potemra, T.A.: Net field-aligned currents observed by Triad. J. Geophys. Res. **81**, 2155–2164, 1976

Sulzbacher, H., Baumjohann, W., Potemra, T.A.: Coordinated magnetic observations of morning sector auroral zone currents with Triad and the Scandinavian Magnetometer Array: a case study. J. Geophys. **48**, 7–17, 1980

Theile, B., Boström, R., Dumbs, A., Grossmann, K.U., Krankowsky, D., Lämmerzahl, P., Marklund, G., Neske, E., Schmidtke, G., Wilhelm, K.: In situ measurements of heating parameters in the auroral ionosphere. Planet. Space Sci. **29**, 455–468, 1981

Untiedt, J., Pellinen, R., Küppers, F., Opgenoorth, H.J., Pelster, W.D., Baumjohann, W., Ranta, H., Kangas, J., Czechowsky, P., Heikkila, W.J.: Observations of the initial development of an auroral and magnetic substorm at magnetic midnight. J. Geophys. **45**, 41–65, 1978

Vickrey, J.F., Vondrak, R.R., Matthews, S.J.: The diurnal and latitudinal variation of auroral zone ionospheric conductivity. J. Geophys. Res. **86**, 65–75, 1981

Vondrak, R.R., Baron, M.J.: A method of obtaining the energy distribution of auroral electrons from incoherent scatter radar measurements. In: Radar probing of the auroral plasma, A. Brekke, ed., pp. 315–330. Oslo: Universitetsforlaget 1977

Vondrak, R.R., Sears, R.D.: Comparison of incoherent scatter radar and photometric measurements of the energy distribution of auroral electrons. J. Geophys. Res. **83**, 1665–1667, 1978

Wallis, D.D., Budzinski, E.E.: Empirical models of height integrated conductivities. J. Geophys. Res. **86**, 125–137, 1981

Wiens, R.G., Rostoker, G.: Characteristics of the development of the westward electrojet during the expansive phase of magnetospheric substorms. J. Geophys. Res. **80**, 2109–2128, 1975

Winningham, J.D., Heikkila, W.J.: Polar cap auroral electron fluxes observed with Isis 1. J. Geophys. Res. **79**, 949–957, 1974

Winningham, J.D., Yasuhara, F., Akasofu, S.-I., Heikkila, W.J.: The latitudinal morphology of 10 eV to 10 keV electron fluxes during magnetically quiet and disturbed times in the 2100–0300 MLT sector. J. Geophys. Res. **80**, 3148–3171, 1975

Yasuhara, F., Kamide, Y., Akasofu, S.-I.: Field-aligned and ionospheric currents. Planet. Space Sci **23**, 1355–1368, 1975

Zi, M., Nielsen, E.: Spatial variations of ionospheric electric fields at high latitudes on magnetic quiet days. In: Exploration of the polar upper atmosphere, C.S. Deehr and J.A. Holtet, eds., pp. 293–304. Dordrecht: D. Reidel, 1980

Received November 11, 1981; Revised version March 3, 1982
Accepted March 17, 1982